KITAIGORODSKY, A. I. (1961). *Organic Chemical Crystallography*. New York: Consultants Bureau.
KITAIGORODSKY, A. I. (1973). *Molecular Crystals and Molecules*. New York: Academic Press.
KITAIGORODSKY, A. I. & MIRSKAYA, K. V. (1962). *Sov. Phys. Crystallogr.* **6**, 408–412.
KITAIGORODSKY, A. I. & MIRSKAYA, K. V. (1964). *Sov. Phys. Crystallogr.* **9**, 137–142.
KITAIGORODSKY, A. I. & MIRSKAYA, K. V. (1965). *Sov. Phys. Crystallogr.* **10**, 121–124.
KITAIGORODSKY, A. I. & MIRSKAYA, K. V. (1972). *Mater. Res. Bull.* **7**, 1271–1280.
LIFSON, S. & WARSHEL, A. (1968). *J. Chem. Phys.* **49**, 5116–5129.
LONSDALE, K., MILLEDGE, H. J. & KRISHNA RAO, K. V. (1960). *Proc. Roy. Soc.* A**255**, 82–100.
MCCALL, D. W. & DOUGLASS, D. C. (1960). *J. Chem. Phys.* **33**, 777–778.
MIRSKAYA, K. V. (1963). *Sov. Phys. Crystallogr.* **8**, 167–168.
MIRSKAYA, K. V. (1973). *Tetrahedron*, **29**, 679–682.
MIRSKAYA, K. V., KOZLOVA, I. E. & BEREZNITSKAYA, V. F. (1974). *Phys. Stat. Sol. (b)*, **62**, 291–294.
MOMANY, F. A., CARRUTHERS, L. M., MCGUIRE, R. F. & SCHERAGA, H. A. (1974). *J. Phys. Chem.* **78**, 1595–1620.
MOMANY, F. A., VANDERKOOI, G. & SCHERAGA, H. A. (1968). *Proc. Natl. Acad. Sci. U.S.* **61**, 429–436.
NORDMAN, C. E. & SCHMITKONS, D. J. (1965). *Acta Cryst.* **18**, 764–767.
NOWACKI, W. (1945). *Helv. Chim. Acta*, **28**, 1233–1242.
PISTORIUS, C. W. F. T. & RESING, H. A. (1969). *Mol. Cryst. Liquid Cryst.* **5**, 353–361.
RAE, A. I. & MASON, R. (1968). *Proc. Roy. Soc.* A**304**, 487–499.
RESING, H. A. (1969). *Mol. Cryst. Liquid Cryst.* **9**, 101–132.
SCHALLAMACH, A. (1939). *Proc. Roy. Soc.* A**171**, 569–578.
STOCKMEYER, R. (1969). *Discuss. Faraday Soc.* **48**, 156–161.
WARSHEL, A. & KARPLUS, M. (1972). *J. Amer. Chem. Soc.* **94**, 5612–5625.
WARSHEL, A. & LIFSON, S. (1970). *J. Chem. Phys.* **53**, 582–594.
WAUGH, J. S. & FEDIN, E. I. (1962). *Sov. Phys. Solid State*, **4**, 1633–1636.
WESTRUM, E. F. JR (1961). *J. Phys. Chem. Solids*, **18**, 83–85.
WILLIAMS, D. E. (1966). *J. Chem. Phys.* **45**, 3770–3778.
WILLIAMS, D. E. (1967). *J. Chem. Phys.* **47**, 4680–4684.
WILLIAMS, D. E. (1970). *Trans. Amer. Cryst. Assoc.* **6**, 21–34.
WILLIAMS, D. E. (1972). *Acta Cryst.* A**28**, 629–635.
WILLIAMS, D. E. (1974). *Acta Cryst.* A**30**, 71–77.

Acta Cryst. (1976). A**32**, 207

The Interpretation of Quasi-kinematical Single-Crystal Electron Diffraction Intensity Data from Paraffins

BY DOUGLAS L. DORSET

Medical Foundation of Buffalo, 73 High Street, Buffalo, New York 14203, *U.S.A.*

(*Received* 12 *June* 1975; *accepted* 17 *October* 1975)

Single-crystal *hk*0 electron diffraction patterns from thin (≤ 240 Å) rhomboid n-hexatriacontane (n-$C_{36}H_{74}$) crystals contain intensity data which are well fit by the commonly observed $O_\perp$ methylene subcell phasing model but not by a true unit cell model which contains two mutually displaced monolayers. The apparent diffraction from a monolayer in these lamellar crystals is thought to be due to bend distortions of the crystal plate. Intensity data conform to a kinematical interpretation as a first approximation, thus allowing *a priori* structural elucidation, but eventually will require an *n*-beam dynamical correction.

Introduction

The elucidation of molecular conformation in the solid state for many biologically interesting long-chain lipids has often been frustrated by the reluctance of such compounds to give crystals of suitable size and quality for conventional crystallographic structural determinations. The veracity of this statement is underscored by the fact that the first three-dimensional X-ray crystal structure analysis of a phospholipid, for example, was completed only recently using three-dimensional X-ray diffraction data of poor quality (Hitchcock, Mason, Thomas & Shipley, 1974).

With the encouragement of pioneering Russian structural work on organic materials, it is believed that the crystal size criterion may be overcome by the use of electron diffraction intensity data from readily available thin microcrystals for the crystallographic analysis of unknown lipid structures. The very small crystal thickness (a hundred ångströms or less) for which one can obtain high-resolution single-crystal diffraction patterns is an expression of the very large scattering cross section of matter for electrons (Vainshtein, 1964, p. 4). This large scattering cross section in itself demands a proof that a given diffraction data set adequately conforms to the kinematical diffraction assumption used in X-ray crystallography and thus allows an *a priori* determination of an unknown crystal structure. Much of the Russian literature on electron diffraction determination of organic crystal structures described the

use of polycrystalline samples, ostensibly to ensure crystallite sizes small enough to satisfy this kinematical criterion which states that no appreciable fraction of the incident electron beam power must be attenuated by the diffraction process (*e.g.* Gevers, 1970, p. 7). All else being equal, single-crystal patterns are preferable to texture patterns in that the latter introduce many more barriers to the determination of unit-cell dimensions and symmetry and also restrict the number of obtainable intensity data (Vainshtein, 1964, pp. 89–103).

For thin single crystals comprised of light atoms there is reason to expect that single-crystal diffraction data should mostly conform to the kinematical diffraction assumption (Cowley & Moodie, 1962) and thus, given a suitable goniometer stage in the electron microscope and adequate protection against radiation damage, one conceivably should be able to obtain a three-dimensional intensity data set from a single lipid crystal suitable for crystallographic analysis. The efficacy of the kinematical approximation for treatment of single-crystal electron diffraction data from lipids has already been demonstrated in the crystallographic analyses of the hexagonal aliphatic chain packing in the high-temperature crystalline forms of a 1,2-diglyceride (Dorset, 1974) and three phospholipids (Dorset, 1975*a*) and the $O_\perp$ methylene packing in a pure ketonic wax secreted by *Prociphilus tessellatus* (Dorset, 1975*b*). Since we are currently engaged in a determination of several other lipid structures using single-crystal electron diffraction data, a model study on paraffins was carried out in order to assess rigorously what conditions are optimal for obtaining kinematical single-crystal diffraction data from these compounds and what corrections must be applied to the best intensity data set.

Materials and methods

Sample preparation

Orthorhombic microcrystals of n-hexatriacontane, n-$C_{36}H_{74}$, (98% pure, Aldrich Chemical Co., Milwaukee, Wisc.) were grown on carbon-Formvar covered Cu° electron microscope grids by evaporation of a dilute solution in light petroleum. Electron micrographs of Au°-shadowed rhomboid crystals (Fig. 1) obtained on a Siemens IA electron microscope (80 kV accelerating voltage) revealed the spiral monomolecular growth characteristic of this compound (Dawson & Vand, 1951). Crystals giving diffraction patterns without forbidden reflections were found to be ≤ 240 Å at their thickest point. This thickness estimate is based on micrographs of crystals on a representative grid (later gold-shadowed) used in diffraction experiments.

Electron diffraction

Electron diffraction experiments were initially carried out at 80 kV ($\lambda = 0{\cdot}04177$ Å) in a Siemens IA electron microscope. Incident beam intensity to the sample was minimized by use of a 20 μm aperture at condenser lens 2. Diffraction patterns were formed in this case by focusing the intermediate lens on the back focal plane of the objective lens. Later experiments were done at 100 kV ($\lambda = 0{\cdot}03702$ Å) in a JEOL JEM-100U electron microscope equipped with a 30° tilt goniometer stage. With this microscope the diffraction patterns were obtained by operating in the selected-area diffraction mode after initial focusing of a representative crystal image from the specimen grid and then searching for diffraction patterns by movement of the translation controls. Beam current at the sample was minimized by use of a 20 μm aperture at condenser lens 2 and by spreading out the beam spot with condenser lens 1. Radiation damage was further minimized by liquid nitrogen cooling of the specimen stage. For all experiments, diffraction patterns were recorded on Kodak no-screen X-ray film which is 17-fold more sensitive than electron image plates at 100 kV (Matricardi, Wray & Parsons, 1972). Diffraction spacings were calibrated by simultaneous recording of single-crystal paraffin and Au° powder diffraction patterns from a region of the specimen grid upon which a thin film of Au° had been evaporated.

Intensity measurements from films

The intensities of the diffraction spots on the photographic films were measured using a Joyce–Loebl MkIII C–S flat-bed microdensitometer. Intensity values were obtained by integrating under peaks in the densitometer traces. Typical widths of low-intensity spots on the films are 200 to 300 μm. In the densitometer scan a slit width *ca* 0·26 μm and a slit height *ca* 1 mm (corresponding to the breadth of the darkest spot) were used.

A large possible source of error is exceeding the linear range of response of the photographic film. Care must be taken to optimize the exposure time to eliminate this. This is done by comparing relative intensities of spots on patterns from a given crystal taken at different exposure times. With this condition satisfied, the error inherent in intensity data measurement from films is given by Wooster (1964). For darkest (200, 110) diffraction spots in these experiments, the greatest error in the average density in a scan is estimated to be around 10% – whereas the error in the density of other spots is less than this. Greater accuracy in the measurement of the darker spots could be obtained by devising an integrating camera setup on the electron microscope (Cowley, 1953) to spread out the diffraction spots. Since the work described here was performed on instruments in other laboratories, there was no freedom to alter the equipment. Furthermore, the use of integrating cameras also tends to convert normally weak reflections into ones which are indistinguishable from the background density on the film (Stout & Jensen, 1968, p. 173).

A source of error not considered here is the effect of inelastically scattered electrons. In this paper we have considered inelastic and elastic scattering to be

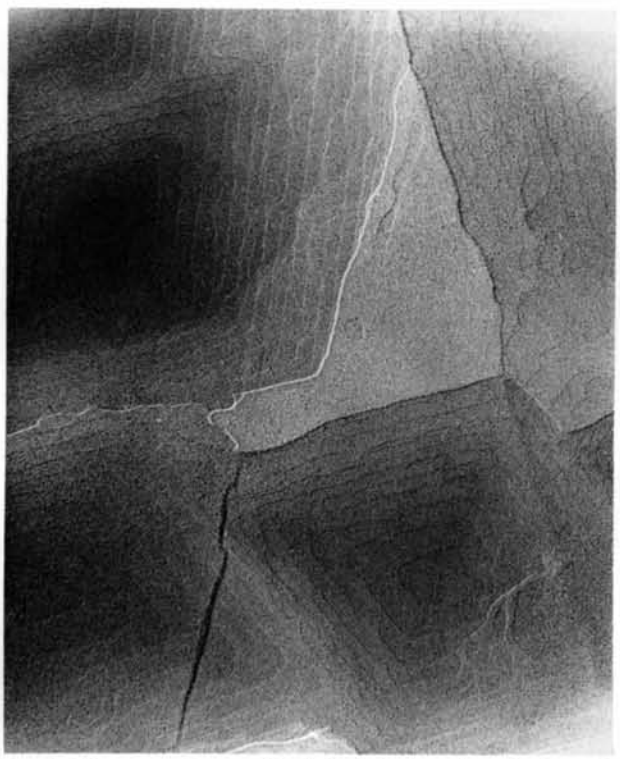

Fig. 1. Electron micrograph of Au°-shadowed orthorhombic n-hexatriacontane single crystals showing spiral growth. Graininess of micrographs is due to clustering of Au° particles. Measured values of the acute angle at the {110} faces give $\chi = 68 \pm 2°$ in comparison to the 67° reported for orthorhombic paraffin crystals (Amelinckx, 1956).

To face p. 208

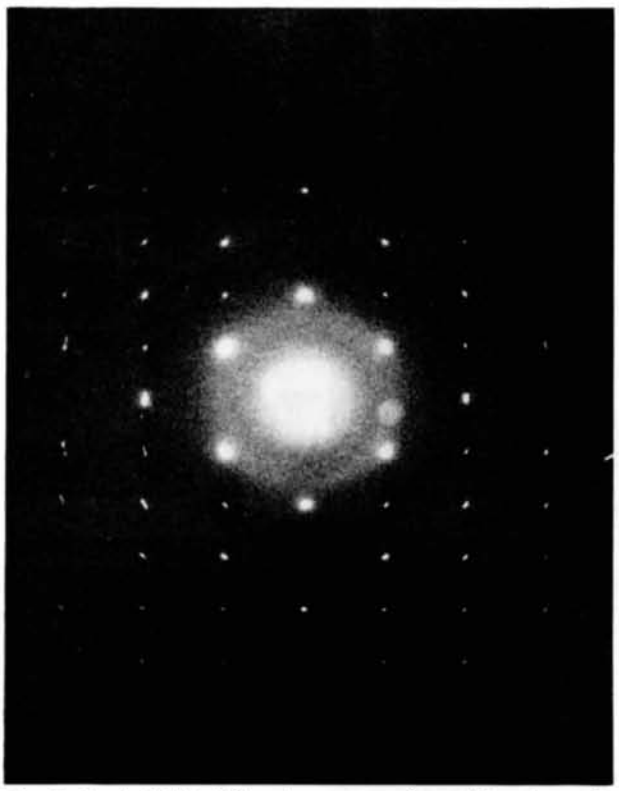

Fig. 2. Typical *hk*0 diffraction pattern from thin n-hexatriacontane crystal (≤ 240 Å).

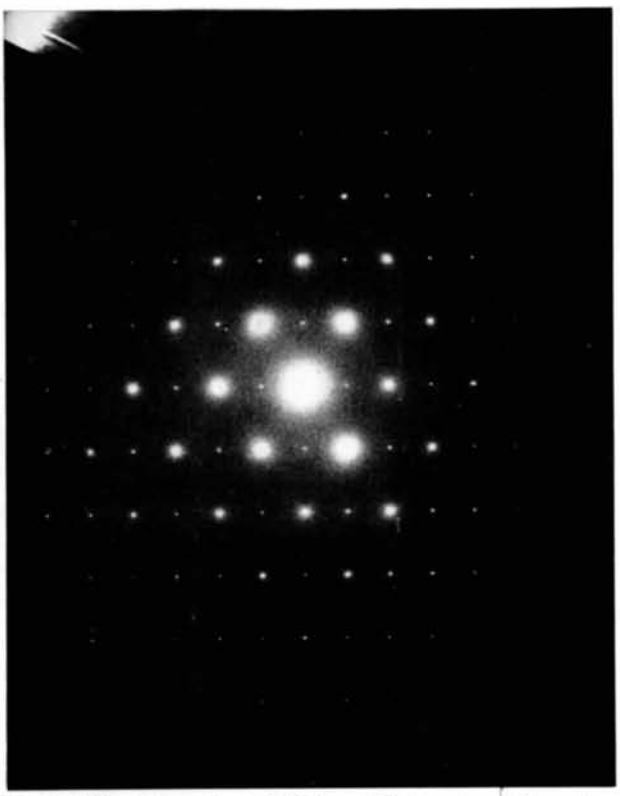

Fig. 3. Diffraction pattern (*hk*0) from thicker n-hexatriacontane crystal showing forbidden reflections along reciprocal axes. Evidence of crystal bending is also seen by violation of *mm* symmetry for large angle spots.

uncorrelated, which, strictly speaking, is an incorrect assumption (*e.g.* Kuwabara, Uefuji & Takamatsu, 1974). It is possible to remove inelastically scattered electrons by any of a number of energy filters (*e.g.* Metherell, 1971) but such apparatus was not available for our use.

Calculations

Structure factor calculations were done with the computer program *LINUS* (Schlemper, Hamilton & LaPlaca, 1971) on a CDC6400 computer using structure factor tables for carbon and hydrogen from Vainshtein's book* (1964, p. 402). Potential maps were generated using phased $|F_{obs}|$ output from *LINUS* in the computer program *JIMDAP* (Schlemper, Hamilton & LaPlaca, 1971). Corrections for multiple scattering and *n*-beam dynamical interactions utilized a computer program for convolution of arrays of delta functions written for a PDP 11/45 computer.

Results and discussion

Diffraction patterns

As shown in Fig. 2, when the crystal thickness is of the order of 240 Å (or less) a characteristic single crystal $O_\perp$ methylene *hk*0 electron diffraction pattern is obtained which is similar to those published elsewhere (Vainshtein, 1964, p. 18; Cowley, Rees & Spink, 1951). The systematic absences along the reciprocal axes indicating plane group *pgg* are particularly striking. The unit-cell spacings calibrated from the internal Au° powder diffraction standard are found to be $a=7{\cdot}37$, $b=4{\cdot}95$ Å and are comparable to previous electron diffraction measurements on n-hexatriacontane (Dawson & Vand, 1951), *viz.* $a=7{\cdot}38$ and $b=4{\cdot}94$ Å. An X-ray structural investigation of this compound by Teare (1959) gave for the orthorhombic form: $a=7{\cdot}42$, $b=4{\cdot}96$, $c=95{\cdot}14$ Å.

As the crystal thickness increases, forbidden reflections appear in the diffraction pattern which are ascribed to multiple scattering (Cowley, Rees & Spink, 1951). An extreme case of this is shown in Fig. 3. Whereas patterns without forbidden reflections are observed to contain data out to $\sin\theta/\lambda \leq 0{\cdot}62$ Å^{-1} at 100 kV, those with forbidden reflections from thicker crystals have been seen to give data out to $\sin\theta/\lambda = 0{\cdot}83$ Å^{-1}. Patterns from similar compounds (such as polyethylene) exhibiting dramatic effects of multiple scattering have been published (Kobayashi & Sakaoku, 1965; Kobayashi, Uyeda & Kawaguchi, 1972) and have been used in structural analysis (Kobayashi, Uyeda & Kawaguchi, 1972).

Derivation of observed structure factor magnitudes

In the derivation of structure factor magnitudes from observed intensities, it is of particular importance to determine what 'Lorentz correction' must be applied to the diffraction data. For electron diffraction from single plate crystals, this is merely an assessment of how much the shape transform of the crystal plate is smeared by mosaicity and what correction must then be made to (higher-angle) data to compensate for an Ewald sphere of finite radius intersecting 'reciprocal lattice rods' away from the position of maximum intensity. Vainshtein (1956) prescribed a multiplication of the intensity by the reciprocal vector length d^*_{hkl} for a given reflection in the case of mosaic crystals, *i.e.*

$$|F^{rel}_{hkl}|^2 = I^{rel}_{hkl} \cdot d^*_{hkl} .$$

As will be discussed in greater detail below, the apparent mosaicity in the paraffin crystals is much more marked in distribution around axes in the plane of the plate than around an axis normal to the plate surface. Therefore, the smearing of the shape transform is so severe that there is no appreciable attenuation of the diffraction intensity as one moves away from the reciprocal lattice point to a reciprocal distance corresponding to a particular deviation parameter s_{hk0} for the Ewald sphere at *hk*0. This is demonstrated in a plot of observed intensities for several diffraction spots in a tilt diffraction series on a single *n*-hexatriacontane microcrystal (Fig. 4). The relevant deviation parameters for 100 kV electrons are given in Table 1.

Table 1. *Deviation parameters for* 100 kV *electrons*

*hk*0	d^*_{hk0} (Å^{-1})	s_{hk0} ($\times 10^3$ Å^{-1})
110	0·2433	1·08
310	0·4545	3·74
200	0·2714	1·33
020	0·4040	2·98
220	0·4866	4·32

Allowing that there is some scatter in the observed intensities due to the sampling of different parts of the crystal plate for successive diffraction patterns in the tilt series, it is still apparent from Fig. 4 that the use of d^*_{hkl} as a Lorentz factor, in this case, is an overcorrection of high-angle data. Indeed, it appears that very little error will result from the assumption: $|F^{rel}_{hkl}|^2 = I^{rel}_{hkl}$ for these crystals.

Crystal structure analysis

For reasons which will be discussed below, the best agreement between the observed *hk*0 structure factors and the calculated structure factors (based on the accepted carbon and hydrogen atomic positions for the $O_\perp$ methylene subcell [Vainshtein, Lobachev & Stasova, 1958; Teare, 1959]) occurs when there is no correction of the calculated structure factors for thermal motion. The observed *hk*0 data for several n-hexatria-

* As was pointed out by a reviewer, it is preferable to use the more accurate atomic scattering factor tables calculated by Doyle & Turner (1968) and tabulated in Volume 4 of *International Tables for X-Ray Crystallography* (p. 155). The greatest error introduced in this present study is <4% in the carbon scattering contribution to the 110 reflection, however, and will not significantly affect the results.

contane crystals are tabulated along with the calculated kinematical structure factors $B=0{\cdot}0$ Å^2 in Table 2. The agreements between the calculated and observed data sets are indicated by the commonly used crystallographic residual defined, as usual, by:

$$R=\frac{\sum||F_{obs}|-k|F_{calc}||}{\sum|F_{obs}|}.$$

Intensity data were taken only from diffraction patterns with *mm* symmetry of the intensity weighted *hk*0 reciprocal net which showed no signs of forbidden reflections along the reciprocal axes.

The X-ray crystal structure determination for orthorhombic n-hexatriacontane (Teare, 1959) indicates the unit cell to be twice the monomolecular thickness with adjacent layers of $O_\perp$ packed chains having their axes displaced from perfect alignment in the (001) projection by symmetry operations of space group $Pca2_1$ (*International Tables for X-ray Crystallography*, 1969). This result differs from ours, and use of atomic x,y coordinates from this determination to calculate structure factors gives a much worse fit to our observed data (*e.g.* $R=0{\cdot}55$ for this model *vs* $R=0{\cdot}29$ for a simple $O_\perp$ subcell packing model for data set #VII in Table 2). The possible meaning of this discrepancy will be discussed in the following section, which evaluates the consequence of elastic bend distortions to the crystal plates.

Two cycles of Fourier refinement are found to shift the carbon and hydrogen atom positions from the input *subcell* coordinates (Teare, 1959) as in Table 3.

Table 2. *Observed vs calculated structure factors for several* n-*hexatriacontane crystals* ($B=0{\cdot}0$ Å^2)

Data sets scaled such that $\sum|F_{obs}|=\sum|F_{calc}|$.

hkl	$\|F_o\|$(I)	$\|F_o\|$(II)	$\|F_o\|$(III)	$\|F_o\|$(IV)	$\|F_o\|$(V)	$\|F_o\|$(VI)	$\|F_o\|$(VII)	F_{calc}
200	6·07	6·55	6·51	6·32	4·80	5·07	5·22	+6·79
400	3·28	3·11	2·95	2·22	3·04	2·43	3·27	+3·12
600	0·64	0·90	0·80			0·79	0·97	+0·87
800							0·64	−0·74
110	6·34	6·89	5·84	7·25	5·89	7·18	7·23	+7·14
210	1·30	1·46	1·84	1·41	1·95	1·54	1·87	−1·48
310	4·18	3·33	3·36	3·20	2·49	2·72	3·94	+2·18
410	1·59	1·74	1·58	0·88	1·04	1·37	1·71	−1·19
510	1·51	1·70	1·33	1·03	1·21	1·32	1·38	+1·21
610	1·21	1·23	1·17	0·76	0·97	0·89	1·07	−1·03
710	0·87	0·68			0·93		0·97	−0·64
810	0·43						0·36	−0·58
910							0·57	−0·82
020	3·24	3·28	4·32	4·41	4·32	4·66	4·13	+4·15
120	1·14	0·75	1·39	1·33	1·31	1·44	1·40	−1·35
220	2·60	2·51	2·31	2·59	2·56	2·35	2·85	+1·38
320	2·06	2·09	1·35	1·99	1·69	1·83	2·42	−1·67
420	1·37	1·32	1·02	1·33	1·31	1·49	1·61	+0·62
520	2·03	1·82	1·76	1·13	1·31	1·32	1·68	−1·50
620	0·75	0·62			0	0·87	0·55	−0·10
720	1·02	0·72			1·04	1·08	1·07	−1·15
820							0·76	−0·94
130	1·51	1·68	1·74	2·37	2·52	2·43	2·09	+2·14
230	1·30	1·35	1·39	1·51	1·61	1·71	1·68	−1·64
330	0·80	1·03	0·90	1·28	1·12	1·30	1·09	+0·77
430	1·61	1·54	1·45	1·21	1·73	1·54	1·64	−1·45
530	0·57	0·54	0	0	0	0·58	0	+0·85
630	1·28	1·31	1·00	0·93	1·16	1·25	1·30	−1·56
730							0	−0·09
830							0·52	−0·81
040	0·49	0·44			1·35	0·58	0·28	+0·84
140	0·69	0·72			1·31	0·34	0·50	−0·95
240	0	0			0·59	0·36	0·47	+0·18
340	1·39	1·24			1·07	0·72	1·00	−1·28
440	0	0					0·57	+0·32
540	1·16	0·96					0·97	−1·52
640							0·36	+0·30
740							0·47	−1·30
150	0·49	0·70					0·45	−0·73
250	0·64	0·68					0·28	−0·96
350	0·69	0·58					0·28	−0·77
450	0·75						0·33	−0·89
Residuals								
F_{calc} ($B=0$)	0·26	0·22	0·19	0·20	0·23	0·21	0·29	
F_{calc} ($B=3$)	0·35	0·31	0·24	0·22	0·32	0·26	0·33	
Φ_{calc} ($B=3$)	0·27	0·23	0·16	0·14	0·25	0·21	0·23	

Table 3. *Shifts in* C *and* H *positions after two cycles of Fourier refinement*

		Input	Cycle 1	Cycle 2
C	*x/a*	0·039	0·034	0·034
	y/b	0·064	0·056	0·056
H(1)	*x/a*	0·181	0·207	0·160
	y/b	0·044	0·035	0·025
H(2)	*x/a*	0·008	0·024	0·038
	y/b	0·274	0·308	0·288

The R value changes only slightly after the first cycle of Fourier refinement (0·23 *vs* 0·24). After the first cycle the determined valence parameters are: C–H_1 = 1·28; C–H_2 = 1·25 Å; H_1–Ĉ–H_2 = 98°. The second cycle gives improved values: C–H_1 = 1·15; C–H_2 = 0·94 Å; H_1–Ĉ–H_2 = 98°. These are compared to values found by Vainshtein, Lobachev & Stasova (1958): C–H = 1·12 Å, H_1–Ĉ–H_2 = 107·8°, and by Teare (1959): C–H = 1·07 Å, H–Ĉ–H = 107°. Potential maps after one cycle of Fourier refinement are shown in Fig. 5. The carbon–carbon bond makes an angle of 42·1° to the b axis and

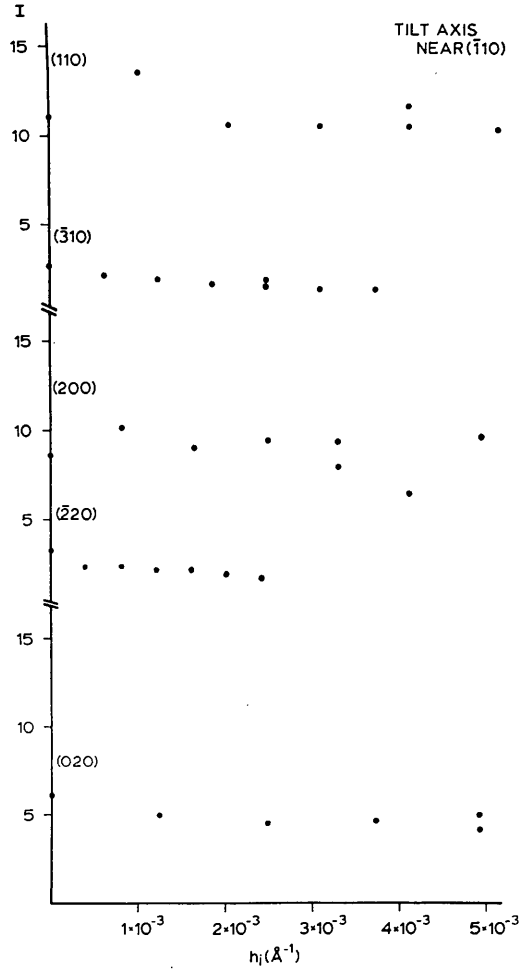

Fig. 4. Observed intensities for strong reflections in tilt series of n-hexatriacontane single crystal from 0° to 1·5° by increments of 0·25°.

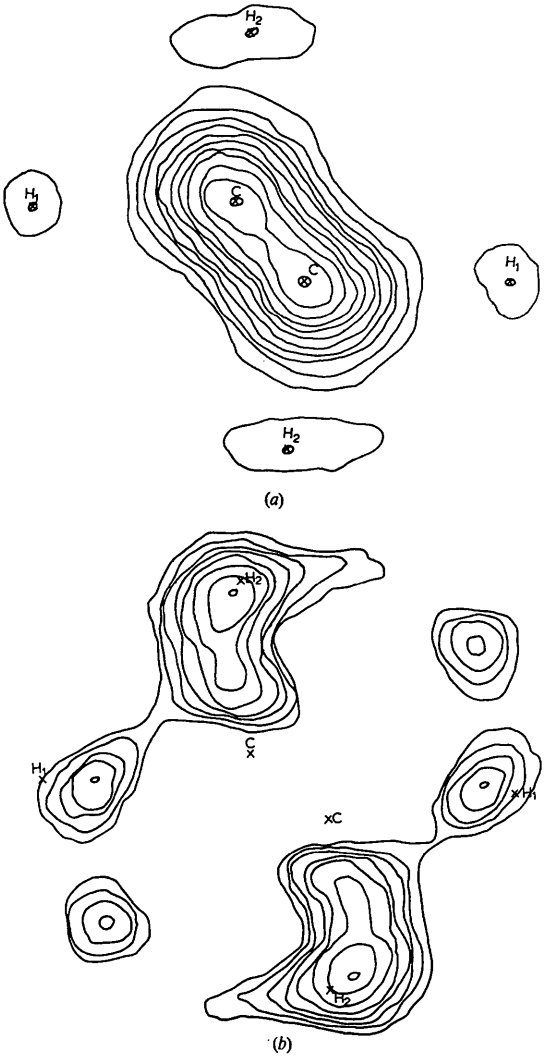

Fig. 5. Potential maps [(001) projection] after one cycle of Fourier refinement (*a*) C,H positions input to structure factor calculations (*b*) difference map with only C position input to structure factor calculation. Data set II used in calculations.

is comparable to the value of 42·3° found by Teare (1959).

Crystal morphology and perfection

It is well documented (Dawson & Vand, 1951) and corroborated by our electron micrographs (*e.g.* Fig. 1) that crystals of *n*-hexatriacontane, as well as those of other normal alkanes (Dawson, 1952; Anderson & Dawson, 1953), grow from screw dislocations arising from slippage of adjacent hydrocarbon chains along the long molecular axis (Dawson, 1952). Were the screw dislocation the only departure from crystal perfection, then one would expect no effect of this disorder in the *hk*0 diffraction pattern since the dislocation slip vector is normal to the {001} face (Hirsch, Howie, Nicholson,

Pashley & Whelan, 1965, pp. 172–174). However, some angular breadth to the diffraction spots (as well as occasional slight arcing of high-angle spots) is observed, which indicates mosaic structure in the {001} plane. In the related case of crystalline polyethylene, moiré fringe patterns observed in dark-field electron micrographs from two nearly parallel overlapped single crystals (Holland, 1964; Sadler & Keller, 1970) have revealed edge dislocations in the {001} plane and, along with low-angle X-ray line-broadening data (Hosemann, Wilke & Balta Calleja, 1966), have been interpreted to represent a mosaic structure with component units of 300 Å lateral diameter and orientational twist about (001) by at least 0·6°. The likely presence of dislocations in the {001} plane producing an array of small scattering domains which are mutually optically incoherent can be a major factor to be considered in the evaluation of what corrections are appropriate to *hk*0 electron diffraction intensities from single paraffin crystals.

Another manifestation of crystal imperfection is the intensity distribution in the *hk*0 diffraction pattern which, as mentioned already, is correlated with the diffraction from a monolayer, but not from the true unit cell. Based on the arguments in the electron diffraction study of the disordered boric acid structure (Cowley, 1953), it was first thought that random stacking disorders cause each monolayer in a paraffin crystal to behave as if optically incoherent from each other one in the lamellar array – for the assumption of direct stacking of chain axes on top of each other to cause a perfectly eclipsed view down [001] is untenable from a consideration of minimized end-plane packing energy for these long-chain compounds (Kitaigorodskii, 1961, pp. 193–207). The observed presence of multimolecular growth steps for thick *n*-hexatriacontane crystals (Dawson & Vand, 1951), which would apparently contain the true bilayer unit cell of contiguous monolayers translated by the symmetry operations of $Pca2_1$, seemed to support this argument.

Yet it is difficult to accept the presence of the large number of stacking disorders required to cause this effect in a single microcrystal since the crystals are often made up of only five layers or less. A much more cogent explanation is the restriction of *thickness* which gives coherent diffraction from crystals having significant bend distortions within the coherence width of the incident electron beam (Cowley, 1961). Such effects were noted in the electron diffraction of some inorganic compounds (Cowley, 1956; Cowley & Ibers, 1956; Cowley & Goswami, 1961) where the symmetry of the electron diffraction patterns was always higher than anticipated from the symmetry of the unit cell and corresponded to packings of single layers in the crystals.

It is known that crystals of these long-chain compounds show bend contours in electron images (Sadler & Keller, 1970). The presence of significant bend distortions would also account for the exaggerated mosaicity apparent in the {110} planes of these paraffin crystals. As crystals grow thicker and physically overcome the stresses imposed by the underlying polymer film on the electron microscope grid, it is expected that rocking curves from tilt diffraction series should reveal the true unit-cell repeat along **c***. This is in fact shown in Fig. 6.

Recently, this argument has been used (Dorset, 1975*c*) to explain the hexagonal symmetry seen in *hk*0 electron diffraction patterns from the high-temperature polymorphic forms of several lipids (Buchheim & Knoop, 1969; Dorset, 1974, 1975*a*; Knoop & Precht, 1975). The hexagonal symmetry is contrasted to the orthorhombic symmetry found in an X-ray diffraction study of the α form of nonadecane (Larsson, 1967) and at first was interpreted (Buchheim & Knoop, 1969; Knoop & Piecht, 1975) to signify the absence of translational displacements between adjacent monolayers in crystals of these compounds.

'Extinction' correction of intensity data

To assume a paraffin to give diffraction data arising as if from a point atom structure with no thermal motion is quite unrealistic. Yet, if one applies a reasonable correction for thermal motion, say $B=3{\cdot}0$ Å^2, the agreement between the observed and calculated structure factors can change from an R value in the 20% range to one in the 30% range (see Table 2). This phenomenological disparity, which indicates the most intense reflection intensities to be related to the kinematical structure factors by a relation approaching $I \propto |F|$, is symptomatic of an 'extinction' effect. When faced with this situation, earlier workers (*e.g.* Lobachev & Vainshtein, 1961; Dvoryankin & Vainshtein, 1960, 1962) applied a two-beam dynamical adjustment to low-angle data. A graphical correction of this type has also been made by Li (1963) for *hk*0 intensity data

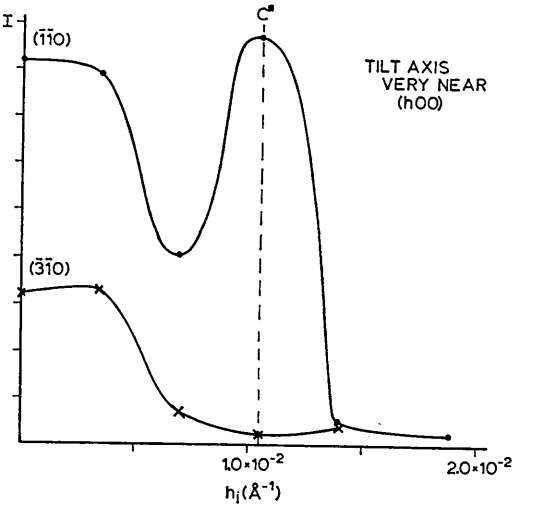

Fig. 6. Rocking curves from tilt diffraction series on a thick n-hexatriacontane microcrystal.

from tricosanol. However, it can be demonstrated that a Darwin (1922) secondary extinction correction works as well as the proposed primary extinction calculations.

The basic flaw in both of these corrections is the assumed independence of all or most diffracted beams. Given the large radius of curvature for the Ewald sphere at 100 kV, this is not a suitable assumption to make – even though there is a strong correlation between observed and calculated structure factors when no isotropic temperature factor is used. In other words, the simultaneous excitation of many beams must not be overlooked.

The effective thickness of the n-hexatriacontane crystals coherently scattering was shown above to be a monolayer or less, *i.e.* $t \leq 47$ Å. Since at 100 kV, $\lambda \,.\, t \leq 1{\cdot}7$ Å^2, the phase-grating approximation to an n-beam dynamical calculation should be valid (Cowley & Moodie, 1962). A propagation function for an electron beam through a thin crystal is given (Cowley & Moodie, 1959) by

$$q(x,y) = \exp\left[i\sigma t\varphi(x,y)\right], \qquad (1)$$

where $\varphi(x,y)$ is the potential distribution for the crystal slice thickness Δz. The constant

$$\sigma = \frac{2\pi}{\lambda \,.\, W \,.\, [1+(1-\beta^2)^{1/2}]},$$

where λ is the relativistic electron wavelength, W is the accelerating voltage and $\beta = v/c$. The exponential in (1) can be expanded:

$$q(x,y) = 1 + i\sigma t\varphi(x,y) - \frac{\sigma^2}{2!}t^2\varphi(x,y)\varphi(x,y) - \frac{i\sigma^3}{3!}t^3\varphi(x,y)\varphi(x,y)\varphi(x,y) + \ldots \qquad (2)$$

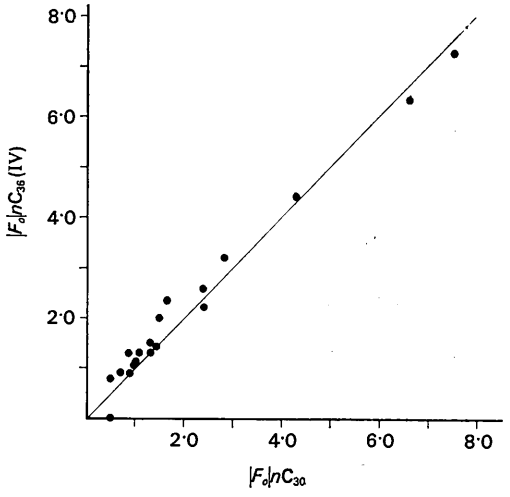

Fig. 7. Cross-correlation of *hk*0 observed structure factors from n-hexatriacontane (single-crystal data IV in Table 2) and n-triacontane (powder data; Vainshtein, Lobachev & Stasova, 1958).

Since the dynamical structure factor Φ_{hk} is obtained by evaluating the Fourier transform of $[q(x,y)-1]$, its magnitude is calculated from:

$$|\Phi_{hk}|^2 = (A+iB)\,(A-iB)\,,$$

where the series

$$A = \frac{\sigma^2}{2!}t^2k^2F^*_{hk}F_{hk} - \frac{\sigma^4}{4!}t^4k^4F^*_{hk}F^*_{hk}F^*_{hk}F_{hk} + \ldots \qquad (3)$$

and

$$B = \sigma tkF_{hk} - \frac{\sigma^3}{3!}t^3k^3F^*_{hk}F^*_{hk}F_{hk} + \frac{\sigma^5}{5!}t^5k^5F^*_{hk}F^*_{hk}F^*_{hk}F^*_{hk}F_{hk} - \ldots \qquad (4)$$

are formed by the Foürier transforms of terms in the expansion (2). For a given structure factor calculation, the series (3) and (4) are expanded until they adequately converge. (The operation * denotes convolution.) The constant $k = 47{\cdot}87/\Omega$ is the conversion of the kinematical structure factors F_{hk} to kinematical potentials V_{hk}.

In the phase-grating calculations for a monolayer of n-hexatriacontane, the diffraction from a stack of $n=18$ $O_\perp$ subcells, $\Delta z = 2{\cdot}54$ Å, such that $t = n \,.\, \Delta z$ was considered. Although no isotropic temperature factor is given in the X-ray crystal structure analysis on the orthorhombic form of n-hexatriacontane (Teare, 1959), Shearer & Vand (1956) use $B = 3{\cdot}0$ Å^2 in their X-ray structural determination for the monoclinic form. A phase-grating calculation using $O_\perp$ subcell F_{hk}'s computed with this temperature factor gave the dynamical structure factor magnitudes shown in Table 4. The close correlation of these values with the observed data is indicated by the residuals in Table 2 which were again calculated after scaling the data such the $\sum|\Phi_{hk}| = \sum|F_{obs}|$.

Table 4. *Dynamical hk*0 *structure factor magnitudes determined for* n-*hexatriacontane using kinematical* $O_\perp F_{hk0}$*'s calculated with* $B = 3{\cdot}0$ Å

Residuals in Table 2, $R = \sum||F_{obs}| - k|\Phi||/\sum|F_{obs}|$, calculated after scaling $\sum|F_{obs}| = \sum|\Phi|$.

hk	$\lvert\Phi_{hk}\rvert$	*hk*	$\lvert\Phi_{hk}\rvert$	*hk*	$\lvert\Phi_{hk}\rvert$	*hk*	$\lvert\Phi_{hk}\rvert$
20	5·78	02	3·31	43	0·97	74	0·41
40	2·16	12	1·07	53	0·33	84	0·10
60	0·42	22	1·70	63	0·75		
80	0·32	32	1·20	73	0·14		
11	6·05	42	0·81	83	0·32		
21	1·24	52	0·96	04	0·49		
31	2·19	62	0·22	14	0·53		
41	0·87	72	0·56	24	0·39		
51	0·77	82	0·36	34	0·72		
61	0·58	13	1·41	44	0·28		
71	0·40	23	1·09	54	0·65		
81	0·26	33	0·64	64	0·10		

It is important to emphasize at this point that structure factor magnitudes determined from texture electron diffraction data are also affected by n-beam inter-

actions. This is demonstrated in Fig. 7 by a cross-correlation of *hk*0 paraffin observed structure factors found in this single-crystal study with those found in an earlier study with crystalline textures (Vainshtein, Lobachev & Stasova, 1958). Even though these texture data are apparently well correlated with the kinematical phasing model (at $B=3{\cdot}0$ Å^2, $R=0{\cdot}21$ for the paraffin mixture; $R=0{\cdot}17$ for $C_{18}H_{38}$; $R=0{\cdot}16$ for $C_{30}H_{62}$), only a phase-grating calculation predicts the attenuation of low-angle reflections such as 200 and 110 and the increase of higher-angle intensities such as 310 and 220.

Correction for multiple scattering

With increasing thickness, the paraffin crystals are observed to produce forbidden odd-order *h*00 and 0*k*0 reflections in the *hk*0 electron diffraction patterns along with diffraction spots extending out to larger values of $\sin\theta/\lambda$. This phenomenon of multiple scattering has been characterized as a kinematical event in mosaic crystals (Vainshtein, 1964, p. 63; Cowley, Rees & Spink, 1951) which arises from intense diffracted beams from one crystallite acting as incident beams for other optically incoherent crystallites in the mosaic.

At least two approaches have been taken to recover the underlying intensity data set, either (*a*) to regard the effects of multiple scattering as a uniformly Gaussian fall-off of intensity in reciprocal space which can be approximated by a plot of forbidden reflection I *vs* $\sin\theta/\lambda$ (Vainshtein, 1964, p. 180) or (*b*) to compensate for the convolution of the diffraction pattern with itself in the case of secondary scattering (Cowley, Rees & Spink, 1951). Considering the latter method, the adjustment for secondary scattering utilizes the expression:

$$I^*_{hk0}=K[I^n_{hk0}-\tfrac{1}{2}f_0tS^n_1/\textstyle\sum^n], \qquad (2)$$

where I^*_{hk0} and I^n_{hk0} are respectively the corrected and observed intensities of *hk*0; S^n_1 accounts for the different diffracted beams of one crystallite acting as primary beams on a second; $\sum^n$ is a sum over all intensities. The product $\frac{1}{2}f_0t$, where f_0 is an attenuating factor for an electron beam through thickness t for elastic scattering, is found by setting $I^*_{hk0}=0$ for forbidden reflections.

Even though the intensity data given by Cowley, Rees & Spink (1951) do not fit the $O_\perp$ methylene phasing model well ($R=0{\cdot}46$ for agreement of F_{obs} and F_{calc} with $B=0{\cdot}0$ Å^2; $R=0{\cdot}37$ for agreement of F_{obs} *vs* F_{calc} with $B=3{\cdot}0$ Å^2), these were used to confirm that our computer program generates results consistent with their calculations.

A self-convolution of paraffin *hk*0 intensities correctly predicts the observation that $I_{100}<I_{300}$ in the case of secondary scattering. The use of the Vainshtein subtraction technique proves to be inappropriate here. For multiple convolutions of the intensities, $I_{100}>I_{300}$ and, given that the number of multiple interactions is still small and that these do not greatly affect the intensity distribution of the diffraction pattern, the simpler Vainshtein correction fortuitously can be used. In general, the method of Cowley, Rees & Spink (1951) appears to be the better model for the phenomenon.

Conclusions

The major conclusion from this study is a reaffirmation of the earlier findings in Vainshtein's laboratory that quasi-kinematical electron diffraction intensity data can often be obtained from thin organic microcrystals and that these data can be used with some success in an *a priori* crystal structure analysis. This result has already been of benefit to our laboratory in uncovering structural information from lipid microcrystals which has so far been inaccessible to X-ray crystallographic analyses.

It must be always recognized, however, that the most rigorous treatment of electron diffraction data is one utilizing an *n*-beam dynamical formulation. Supposed *a posteriori* corrections to either the observed or calculated structure factors which assume any independence of diffracted beams are spurious, even though they may fortuitously improve the fit between data sets. It is also shown that dynamical effects will persist in texture intensity data from light-atom structures.

It is important to emphasize the imperfections inherent in the paraffin crystals. Bend distortions (which are anticipated to be visualized in electron micrographs taken at low beam currents) effectively narrow the crystal thickness giving coherent scattering (to at most a monolayer) such that diffraction from the true unit cell is not seen. The generality of this phenomenon is indicated by parallel studies on orthorhombic microcrystals of n-hexacosane which give the same result. Heightened mosaicity in the {110} crystal planes smears the diffraction spot enough so that Vainshtein's Lorentz correction for mosaic crystals is an overcorrection here.

Mosaicity in the {001} plane caused by edge dislocations (assuming the analogous observation in polyethylene to apply), in addition to the single-layer scattering, is responsible for multiple elastic scattering evidenced by forbidden reflections in diffraction patterns from thick crystals. This has already been adequately stated by Cowley, Rees & Spink (1951) but must be re-emphasized since some recent work (*e.g.* Thomas, Sass & Kramer, 1974) insists that such forbidden reflections in the case of solution-grown polyethylene microcrystals are indicative of crystal perfection.

Previous workers (*e.g.* Gjønnes & Moodie, 1965) have already described the retention of symmetry in the zonal diffraction pattern when the incident beam is parallel to a major crystallographic axis – even when there are strong dynamical effects. This can be conviently demonstrated by any *n*-fold self-convolution of input-phased F's from a centrosymmetric zone of plane group *pgg* which always gives an array N_{hk} with values equal to zero at Miller indices corresponding to space-group-forbidden reflections. Of course, such is not the case for input intensities, which are all positive mag-

nitudes. As shown before, the self-convolution of intensities models multiple scattering and gives space-group-forbidden reflections even when the beam is parallel to the zonal axis. Given also the difficulty in recovering the underlying diffraction pattern which is self-convoluted n times by the multiple scattering process, it is probably not safe even to use Patterson syntheses for structural work, as has been done with polyethylene $hk0$ electron diffraction patterns with strong evidence of multiple diffraction (Kobayashi, Uyeda & Kawaguchi, 1972). There is no way to avoid using very thin crystals to obtain undistorted transmission electron diffraction intensity data.

We are very grateful for a helpful correspondence with Professor J. M. Cowley, who directed our attention to the diffraction work on bend-distorted crystals. Thanks are also due to Dr Donald F. Parsons for permission to use the Siemens Ia electron microscope and Joyce-Loebl MkIIICS microdensitometer in the Electron Optics Laboratory at Roswell Park Memorial Institute, and to Dr S. Ramalingam for permission to use the JEOL JEM-100U electron microscope in the Department of Mechanical Engineering at State University of New York at Buffalo. The electron microscope laboratory at SUNYAB was funded by the National Science Foundation and the New York State Science and Technology Foundation. Electron micrographs of single crystals were obtained by Miss Cynthia M. Strozewski. Research was funded by Public Health Service Grant No. GM 21047 from the National Institute of General Medical Sciences.

References

AMELINCKX, S. (1956). *Acta Cryst.* **9**, 217–224.
ANDERSON, N. G. & DAWSON, I. M. (1953). *Proc. Roy. Soc.* A**218**, 255.
BUCHHEIM, W. & KNOOP, E. (1969). *Naturwissenschaften*, **56**, 560–561.
COWLEY, J. M. (1953). *Acta Cryst.* **6**, 522–529.
COWLEY, J. M. (1956). *Acta Cryst.* **9**, 391–396.
COWLEY, J. M. (1961). *Acta Cryst.* **14**, 920–927.
COWLEY, J. M. & GOSWAMI, A. (1961). *Acta Cryst.* **14**, 1071–1079.
COWLEY, J. M. & IBERS, J. A. (1956). *Acta Cryst.* **9**, 421–431.
COWLEY, J. M. & MOODIE, A. F. (1959). *Acta Cryst.* **12**, 360–367.
COWLEY, J. M. & MOODIE, A. F. (1962). *J. Phys. Soc. Japan*, **17**, (suppl. B-II), 86–91.
COWLEY, J. M., REES, A. L. G. & SPINK, J. A. (1951). *Proc. Phys. Soc.* A**64**, 604–619.
DARWIN, C. G. (1922). *Phil. Mag.* **43**, 800–829.
DAWSON, I. M. (1952). *Proc. Roy. Soc.* A**214**, 72–79.
DAWSON, I. M. & VAND, V. (1951). *Proc. Roy. Soc.* A**206**, 555–562.
DORSET, D. L. (1974). *Chem. Phys. Lipids*, **13**, 133–140.
DORSET, D. L. (1975*a*). *Biochim. Biophys. Acta*, **380**, 257–263.
DORSET, D. L. (1975*b*). *Chem. Phys. Lipids*, **14**, 291–296.
DORSET, D. L. (1975*c*). *Naturwissenschaften*, **62**, 343–344.
DOYLE, P. S. & TURNER, P. S. (1968). *Acta Cryst.* A**24**, 390–397.
DVORYANKIN, V. F. & VAINSHTEIN, B. K. (1960). *Sov. Phys. Crystallogr.* **5**, 564–574.
DVORYANKIN, V. F. & VAINSHTEIN, B. K. (1962). *Sov. Phys. Crystallogr.* **6**, 765–772.
GEVERS, R. (1970). *Modern Diffraction and Imaging Techniques in Material Science*, edited by S. AMELINCKX, R. GEVERS, G. REMAUT & J. VAN LANDUYT. Amsterdam: North Holland.
GJØNNES, J. & MOODIE, A. F. (1965). *Acta Cryst.* **19**, 65–67.
HIRSCH, P. B., HOWIE, A., NICHOLSON, T. B., PASHLEY, D. W. & WHELAN, M. J. (1965). *Electron Microscopy of Thin Crystals*. London: Butterworths.
HITCHCOCK, P. B., MASON, R., THOMAS, K. M. & SHIPLEY, G. G. (1974). *Proc. Natl. Acad. Sci.* U.S. **71**, 3036–3040.
HOLLAND, V. F. (1964). *J. Appl. Phys.* **35**, 3235–3241.
HOSEMANN, T., WILKE, W. & BALTA CALLEJA, F. J. (1966). *Acta Cryst.* **21**, 118–123.
International Tables for X-ray Crystallography, (1969). Vol. 1, p. 115; (1974). Vol. 4. p, 155. Birmingham: Kynoch Press.
KITAIGORODSKII, A. I. (1961). *Organic Chemical Crystallography*. New York: Consultant's Bureau.
KNOOP, E. & PRECHT, D. (1975). *Naturwissenschaften*, **62**, 37.
KOBAYASHI, K. & SAKAOKU, K. (1965). *Lab. Invest.* **14**, 1096–1114.
KOBAYASHI, K., UYEDA, N. & KAWAGUCHI, A. (1972). U.S. Japan Joint Seminar on the Polymer Solid State, Cleveland, Ohio, pp. 188–198.
KUWABARA, S , UEFUJI, T. & TAKAMATSU, Y. (1974). *Proc. Eighth Internat. Congr. E. M.* (Canberra, Australia). Vol. 1, 370–371.
LARSSON, K. (1967). *Nature, Lond.* **213**, 383–384.
LI FAN-KHUA. (1963). *Acta Phys. Sin.* **19**, 735–740.
LOBACHEV, A. N. & VAINSHTEIN, B. K. (1961). *Sov. Phys. Crystallogr.* **6**, 313–317.
MATRICARDI, V. Y., WRAY, G. P. & PARSONS, D. F. (1972). *Micron*, **3**, 526–539.
METHERELL, A. J. F. (1971). *Advanc. Opt. Electron Microsc.* **4**, 263–360.
SADLER, D. M. & KELLER, A. (1970). *Kolloid Z. Z Polym.* **239**, 641–654.
SCHLEMPER, E. O., HAMILTON, W. C. & LAPLACA, S. J. (1971). *J. Chem. Phys.* **5**, 3990–4000.
STOUT, G. H. & JENSEN, L. H. (1968). *X-ray Structure Determination. A Practical Guide*. New York: Macmillan.
TEARE, P. W. (1959). *Acta Cryst.* **12**, 294–300.
THOMAS, E. L., SASS, S. L. & KRAMER, E. J. (1974). *J. Polym. Sci. Polym. Phys. Ed.* **12**, 1015–1022.
VAINSHTEIN, B. K. (1956). *Sov. Phys. Crystallogr.* **1**, 15–21.
VAINSHTEIN, B. K. (1964). *Structure Analysis by Electron Diffraction*. Oxford: Pergamon.
VAINSHTEIN, B. K., LOBACHEV, A. N. & STASOVA, M. M. (1958). *Sov. Phys. Crystallogr.* **3**, 452–459.
WOOSTER, W. A. (1964). *Acta Cryst.* **17**, 878–882.